CHEMISTRY
A EUROPEAN JOURNAL

FULL PAPER

DOI: 10.1002/chem.201103855

Wide-Range Light-Harvesting Donor–Acceptor Assemblies through Specific Intergelator Interactions via Self-Assembly

Suman K. Samanta[a] and Santanu Bhattacharya*[a, b]

Abstract: We have synthesized two new low-molecular-mass organogelators based on tri-*p*-phenylene vinylene derivatives, one of which could be designated as the donor whereas the other one is an acceptor. These were prepared specifically to show the intergelator interactions at the molecular level by using donor–acceptor self-assembly to achieve appropriate control over their macroscopic properties. Intermolecular hydrogen-bonding, π-stacking, and van der Waals interactions operate for both the individual components and the mixtures, leading to the formation of gels in the chosen organic solvents. Evidence for intergelator interactions was acquired from various spectroscopic, microscopic, thermal, and mechanical investigations. Due to the photochromic nature of these molecules, interesting photophysical properties, such as solvatochromism and *J*-type aggregation, were clearly observed. An efficient energy transfer was exhibited by the mixture of donor–acceptor assemblies. An array of four chromophores was built up by inclusion of two known dyes (anthracene and rhodamine 6G) for the energy-transfer studies. Interestingly, an energy-transfer cascade was observed in the assembly of four chromophores in a particular order (anthracene-donor-acceptor-rhodamine 6G), and if one of the components was removed from the assembly the energy transfer process was discontinued. This allowed the build up of a light-harvesting process with a wide range. Excitation at one end produces an emission at the other end of the assembly.

Keywords: chromophores · donor–acceptor systems · energy transfer · gels · reversible reactions

Introduction

Natural photosynthesis occurs with the absorption of sunlight and the manifestation of a continuous unidirectional energy transfer process between chromophores plays a significant role in the efficient light-harvesting process.[1] The organization of dye assemblies at suitable distances and in a specific orientation triggered by noncovalent interactions is responsible for the fast migration of excitation energy.[2] The phenomena of natural-light harvesting are best understood through synthetically designed molecular systems in which supramolecular interactions play a significant role in the chromophore assembly in appropriate orientations.[3] The supramolecular assemblies used to design artificial light-harvesting systems include molecular arrays,[4] supramolecular complexes,[5] dendrimers,[6] and light-harvesting antennae.[7] This self-assembly process is not only important for addressing fundamental questions in the energy-transfer process but is also of great interest in developing advanced materials, including optoelectronic devices, organic light emitting diodes (OLEDs), and solar cells.[8] Thus, developing light-harvesting systems comprised of suitable chromophore arrays holds considerable potential and challenge for emerging new directions.

The supramolecular self-assembly of low-molecular-mass gelators (LMMG)[9] gives rise to physical gels that provide an exceptional opportunity to assist the energy-transfer process.[10] The self-assembly brought about by dipole–dipole, hydrogen-bonding, van der Waals, and π-stacking interactions between appropriate chromophoric molecules provide a novel chromophore assembly.[11] Interesting photophysical properties were observed in oligo(*p*-phenylene vinylene)-based chromophores and research to this end has been spearheaded by Meijer[12] and Ajayaghosh et al.[13] A number of cases has been studied by using synthetic donors and acceptors to modify the efficiency of energy transfer mostly in binary composites.[14] However, there are relatively few chromophore arrays containing more than two molecules interacting through noncovalent interactions that lead to energy transfer mentioned in the literature.[15] Herein, we discuss the donor–acceptor interactions in terms of hydrogen bonding and energy transfer between two new organogelators (**D** and **A**, Scheme 1) based on a central tri(*p*-phenylene vinylene) (TPV) moiety. As per the proposed model reported earlier,[16] we successfully demonstrate herein an extended energy-transfer array that depends on the choice

[a] Dr. S. K. Samanta, Prof. Dr. S. Bhattacharya
Department of Organic Chemistry
Indian Institute of Science
Bangalore 560012, Karnataka (India)
Fax: (+91) 80-23600529
E-mail: sb@orgchem.iisc.ernet.in

[b] Prof. Dr. S. Bhattacharya
Chemical Biology Unit
Jawaharlal Nehru Centre for Advanced Scientific Research
Bangalore 560064, Jakkur (India)

Supporting information for this article is available on the WWW under http://dx.doi.org/10.1002/chem.201103855.

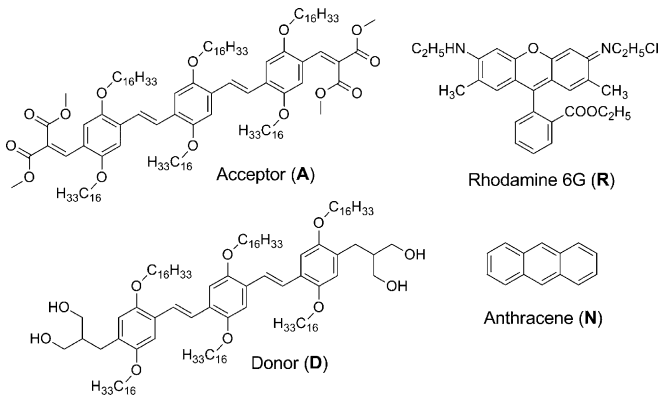

Scheme 1. Molecular structures of TPV gelators (**A** and **D**) and commercially available dyes (**N** and **R**).

of the initial donor and final acceptor coupled with TPV chromophores to manifest an efficient and wide range of light harvesting. We have reported herein the self-assembly properties of the gelators alone or their mixtures composed of the TPV backbone, and the intergelator interactions were probed by using several physical methods, including a number of microscopic and spectroscopic techniques. Also, a cascade energy transfer was observed for assorted chromophore assemblies containing four different luminescent compounds, for example, anthracene, **D**, **A**, and rhodamine 6G. It has been shown that when one of the components was removed from the assembly, the energy transfer process was discontinued.

Results and Discussion

The present investigation includes the synthesis of two new organogelators based on the TPV moiety. They contain the same basic backbone and differ only at the termini, and demonstrate intergelator interactions through hydrogen-bonding, π-stacking, and van der Waals interactions. This leads to the build up of an array with an assembly of different chromophores for light harvesting, based on their donor/acceptor properties.

Synthesis: Lipophilic TPV derivatives **A** and **D** were synthesized in high yields by using a one-step procedure (Scheme S1 in the Supporting Information) starting with the TPV-based bis-aldehyde (**1**) prepared according to a reported procedure.[17] The aldehyde moieties at the end functional groups provide an opportunity to attach functionalities through coupling with active methylene compounds. Thus **A** was obtained through a base-catalyzed Knoevenagel reaction of **1** with dimethyl malonate (DMM). Reduction of **A** by using lithium aluminum hydride afforded tetra alcohol **D**. Each compound was adequately characterized by FTIR, ^{1}H and ^{13}C NMR spectroscopy, MALDI-TOF mass spectroscopy, and elemental analysis (for details see the Experimental Section in the Supporting Information).

Gelation studies: The gelation efficiency of compounds **A** and **D** was studied in different aliphatic and aromatic hydrocarbon solvents. It has been observed that aliphatic hydrocarbon solvents, such as *n*-hexane, *n*-heptane, and *n*-dodecane, could only gelate **A** (minimum gelator concentration (MGC) 2.22 mM in *n*-heptane). However, compound **D** could not be gelated in aliphatic hydrocarbons. This may be due to the presence of four polar OH moieties, which lead to precipitation on cooling after solubilization in alkanes. In contrast, in aromatic hydrocarbons such as toluene, compound **A** did not form a gel but **D** formed a physical gel (MGC≈19.46 mM in toluene). The MGC was high for **D** presumably because of the flexible section between the OH and the aromatic moiety, which may not allow optimum
hydrogen-bonding interactions between molecules of **D**. The van der Waals and aromatic π-stacking interactions are common for both the molecular assemblies. An interesting situation arose when the gelation was attempted by using a mixture of **A**+**D** (1:1 molar ratio; denoted as **C**), which failed to form a gel in toluene but was able to form a gel in aliphatic hydrocarbons such as *n*-heptane (MGC≈5.57 mM). This demonstrates evidence of interactions between **A** and **D** that lead to the gelation of **D** with the aid of **A** in *n*-heptane. All the gels were translucent in nature (Figure S1 in the Supporting Information). The toluene gel of **D** appeared greenish-yellow in color and a brownish-yellow color was observed for the *n*-heptane gel of both **A** and **C** under normal daylight. Under $\lambda = 365$ nm UV light, the toluene gel of **D** showed a sky-blue emission, whereas the *n*-heptane gels derived from **A** and **C** both showed yellow emission.

The gelator **D** has four hydroxyl groups that can serve as hydrogen-bonding donors and gelator **A** has four ester moieties that could act as hydrogen-bonding acceptors. Thus, a mixture of **A** and **D** in 1:1 molar ratio could form a gel; the gelation also persisted when we varied the ratio to 2:1 (**A**/**D**). However, the gelation did not occur when **D**:**A** was mixed in a 2:1 ratio. This again indicates the crucial role of the complementary hydrogen-bonding motifs between **A** and **D**.

The optimized structures (B3LYP, 6-31G*) of **A** showed a *syn* orientation among the two carbonyl groups in the ester moieties at one terminal and it was preferred over the *anti* orientation (Figure S2 in the Supporting Information). Two adjacent carbonyl groups in the *syn* orientation are positioned perpendicular to each other to avoid dipolar repulsion. The *syn* orientation of the two OH groups in gelator **D** was observed to be more stable due to the internal stabilization by hydrogen bonding than the *anti* conformation. The energy profile diagram shows that **A** is energetically more stable due to the greater resonance stabilization energy compared to **D**. However, none of the optimized structures show complete planarity in the conjugated chromophoric part. Thus in the composite, gelators **A** and **D** might adopt a *syn* conformation to give better interaction between them through intermolecular hydrogen-bonding, π-stacking, and van der Waals interactions.

IR spectroscopy studies: FTIR spectral investigations probing the existence of hydrogen-bonding interaction between **A** and **D** were performed to determine the proximity of both the gelators in the composite forming the self-assembly. The IR spectra were recorded for the preformed gel in *n*-heptane for **A** and in toluene for **D** and were compared with the corresponding sol in chloroform. When the spectrum of gelator **A** was recorded in chloroform and compared with the gel samples of **A** in *n*-heptane, the vibrational frequencies due to carbonyl group did not show any significant shift and appeared at 1733 cm^{-1} in both spectra (Figure 1).

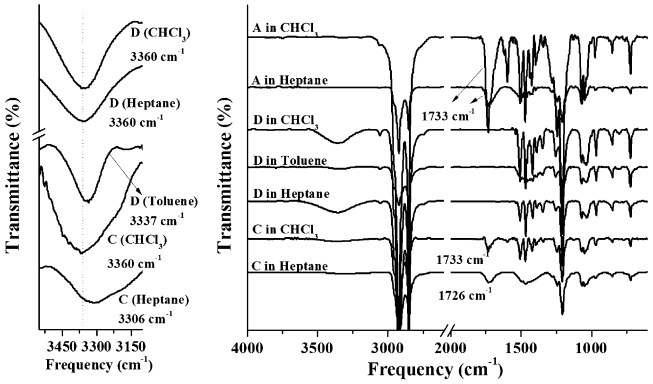

Figure 1. FTIR spectra of **A**, **D**, and **C** in different solvents showing the effect of hydrogen-bonding interactions.

However, the O–H stretching frequency of **D** appeared at 3360 cm^{-1} in chloroform, whereas **D** in toluene as a gel showed a broad O–H stretching band at 3337 cm^{-1}. Therefore, a 23 cm^{-1} shift was observed, which indicates a gel formation induced by hydrogen bonding. Composite **C** showed a stretching frequency due to the O–H function at 3360 cm^{-1} in chloroform. This shifted to 3306 cm^{-1} when the gel of **C** in *n*-heptane was probed under IR. Thus, a pronounced 54 cm^{-1} shift in the IR stretching frequency in the gelation of the composite was observed, which indicates the existence of strong hydrogen-bonding interactions between **A** and **D** in the gel. A lower value in the stretching frequency may be due to the nature of the hydrogen bonding in the mixture, in which the hydrogen bonding of the carbonyl group of **A** with the OH group of **D** could be expected. However, the IR stretching frequency for the carbonyl group showed a change of approximately 6 cm^{-1}. This type of weak hydrogen-bonding interaction between the terminal functional groups of the organogelators is necessary to anchor the formation of the self-assembly.[18] This was further assisted by the π–π interactions between the aromatic backbones of TPV and the van der Waals interactions between the long lipophilic chains of the gelators (Figure S3 in the Supporting Information).[17b]

Rheological studies: The oscillatory stress amplitude of the gels of **A** in *n*-heptane or **D** in toluene showed greater values for the elastic modulus (G') than the viscous modulus (G'') by an order of magnitude, which indicates a dominant elastic behavior (stiffness), that is, resistance to flow under applied stress (Figure 2).[19] The oscillatory frequency response of the gels reveals that G' is independent of the applied angular frequency and much higher than G'' over an angular frequency range of 0.5 to 100 rad s^{-1} (Figure S4 in the Supporting Information). It appears that the gel of **A** in *n*-heptane is mechanically more viscoelastic than the gel of **D** in toluene. The viscoelasticity of the individual gels were not abolished in the donor–acceptor composite (**D**+**A**), as shown by the oscillatory rheological measurements. Under applied angular frequency or shear stress, the solid-like behavior (G') of composite **C** decreased as the percentage of **D** was increased. The yield stress (σ_y), which is an applied stress above which the gel starts to flow, also decreased as the amount of **D** in the composite was increased.

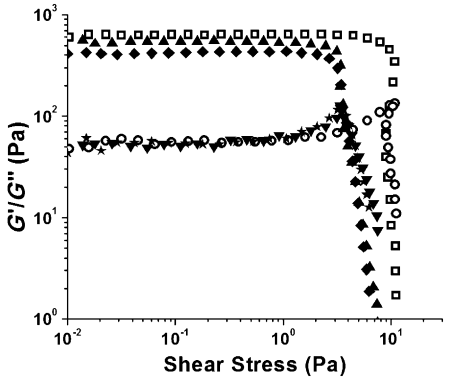

Figure 2. Rheological studies showing the oscillatory amplitude sweep experiment of **A** in the presence of different amounts of **D** (total concentration fixed at 10 mg mL^{-1} in *n*-heptane). □: G' (**A**), ○: G'' (**A**), ▲: G' (**A**/**D**, 2:1), ▼: G'' (**A**/**D**, 2:1), ◆: G' (**A**/**D**, 1:1), ★: G'' (**A**/**D**, 1:1).

Differential scanning calorimetry (DSC) and polarized optical microscopy (POM): The thermotropic behavior of the gels of **A** and **C** in *n*-heptane were investigated to reveal the influence of the interaction on the self-assembly process. The gel-to-sol transition temperature (T_m) did not show any significant changes for either gel (Figure 3). However, a 3 °C decrease in the sol-to-gel transition temperature was observed for **C** compared to **A** alone. Thus, doping with **D** did not significantly alter the thermal stability of **A** in the composite gel. A small decrease in T_m may be accounted for by the additional hydrogen-bonding interactions between **D** and **A**.

The decrease in the melting and solidification temperature was also observed in **C** when examined by using solid-phase DSC (Figure S5 in the Supporting Information). In the heating cycle **A** and **C** showed sharp melting behavior but **D** showed a broad melting transition. The melting temperatures of **A** and **C** did not show any significant changes. However, the solidification of **C** from its molten state took place at a slightly lower temperature (≈2 °C) than that of **A** alone.

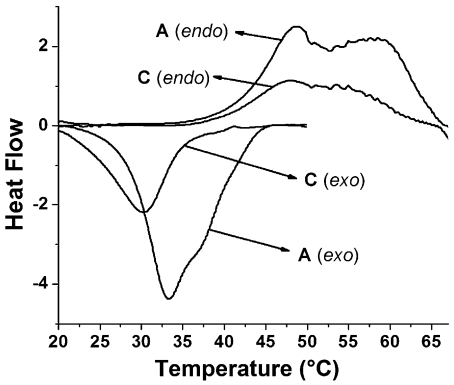

Figure 3. DSC thermograms of the gels of **A** and **C** in *n*-heptane at a final concentration of 8 mM.

Samples **A**, **D**, and their mixtures were optically birefringent at progressively decreasing temperatures from the isotropic melt under a polarized optical microscope. This indicated the anisotropic growth of the gelator molecules in three dimensions to give rise to different birefringent textures.[20] POM images show a greenish-yellow texture with smaller domain size for **D** and a bigger red-colored domain texture of for **A** (Figure S5 in the Supporting Information). However, a smaller red-colored domain texture was observed for **C** when cooled from the isotropic melt. Thus, the texture in **C** was governed by **D**, most likely due to the hydrogen-bonding interactions, and the color was induced by **A**.

Microscopic organization: Various microscopic studies were undertaken to observe the morphology in the individual gel components and the mixture after self-organization. The luminescent nature of the gelator molecules allowed us to observe the superstructures created in a thin film on a glass slide under a fluorescence microscope.[20] When excited by using UV irradiation ($\lambda = 340$–400 nm), the fibers in the thin film showed greenish-yellow emission for **D** and brownish-yellow emission for **A** and **C** (Figure S6 in the Supporting Information). The presence of three-dimensional aggregates was clearly observed in all instances. Notably, in the case of **D** smaller fibers were observed throughout the sample along with the presence of rod-like structures that could form through the assembly of the smaller fibers. Also, a smaller fiber-like morphology was observed in both **A** and **C**. In **C**, the color was similar to **A**, which is a probable consequence of the energy transfer from **D** to **A**.

Transmission electron microscopy (TEM) images showed greater compactness in the aggregated fibers in **C** compared with **D** and **A** (Figure S7 in the Supporting Information). A honeycomb-like structure was observed in all instances. The diameter of the fibers were comparatively uneven in **D** and **A** (50–100 nm) compared with **C**. Also, the fiber diameter increased in the composite (≈ 200 nm) and fibers were organized almost uniformly throughout the sample.

Atomic force microscopy (AFM) images showed the existence of fibrillar networks in both **A** and **D** (Figure 4). Comparatively thinner fibers with diameters of approximately 250 nm were observed in **D**, compared with diameters approximately equal to 1 μm for fibers of **A**. However, the fibrous nature disappeared completely and an aggregated morphology appeared in **C**, which indicated the intergelator interactions.

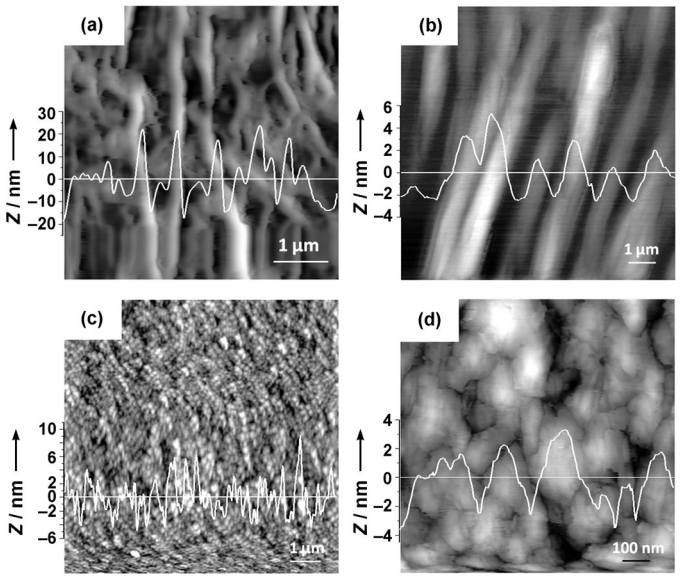

Figure 4. AFM topography images of a) **D**, b) **A**, and c,d) **C**. The embedded graph in each image shows the respective cross-section height profile.

UV/Vis and fluorescence studies: This class of molecule is chromophoric, which allowed evaluation of their photophysical properties.[21] The ground-state interactions between **A** and **D** in the solution phase were examined by using UV/Vis studies in both *n*-heptane and toluene. The absorption maxima (λ_{max}) of **D** and **A** (1×10^{-5} M for both) in *n*-heptane was observed at $\lambda = 402$ and 442 nm, respectively (Figure 5a). Interestingly, composite **C** with a 1:1 molar ratio of **D** and **A** (0.5×10^{-5} M each) in *n*-heptane did not show two different bands but merged to a single band at $\lambda = 427$ nm, which indicated that the individual bands were approximately averaged out in **C**. On increasing the concentration of **D** and **A** (1×10^{-5} M each), the intensity of the absorption band increased without showing any shift in the λ_{max}. Similar absorption spectra were obtained in toluene, with a redshift of 6 nm for both **D** ($\lambda = 408$ nm) and **A** ($\lambda = 448$ nm); the band for **C** appeared at $\lambda = 431$ nm (Figure S8a in the Supporting Information).

When we increased the concentration of one component while keeping the other fixed, a stepwise shift in the λ_{max} with a concomitant increase in the intensity was observed, probably as a consequence of mutual interactions between **D** and **A** (Figure S9 in the Supporting Information). A plot of either absorbance or λ_{max} as a function of the ratio of **D** to **A** showed a crossover at the ratio of 1:1 (**D**:**A**) in both situations, irrespective of whether **A** was titrated with **D** or

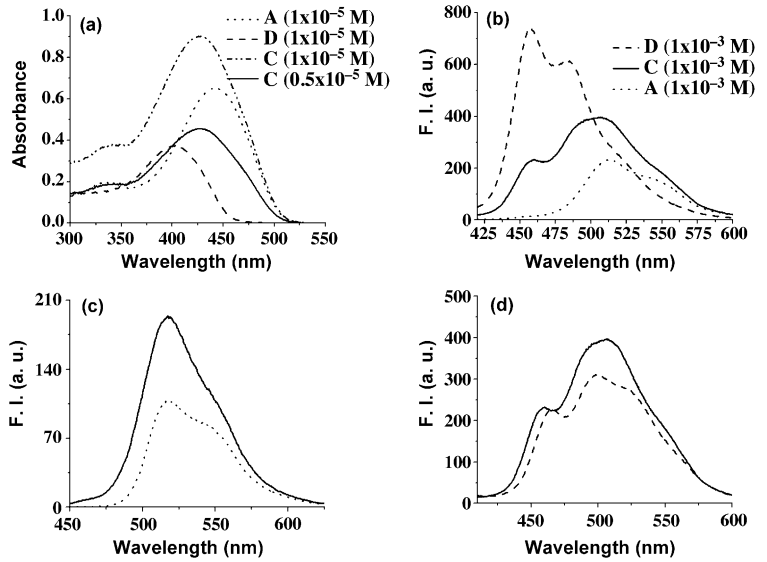

Figure 5. a) Absorption and b) emission spectra of **D**, **A** and **C** in *n*-heptane (excitation at $\lambda = 380$ nm, the concentration of **C** indicates **D**/**A** is 1:1). c) Emission of **C** on excitation at $\lambda = 380$ nm (——) and direct excitation of **A** at $\lambda = 420$ nm (-----) illustrating amplified emission. d) Emission spectra of **C** (1×10^{-5} M) in *n*-heptane (——) and toluene (-----).

D was titrated with **A**. The absorption maxima in **C** did not show two different peaks at the positions of individual chromophores of **D** and **A**, but they appeared to be almost a single component, which indicated the existence of mutual interactions between **D** and **A** in the ground state.

The emission maximum of **D** (1×10^{-5} M) in *n*-heptane appeared at $\lambda = 457$ nm with a hump at $\lambda = 484$ nm; for **A** the maximum was at $\lambda = 512$ nm with a hump near $\lambda = 550$ nm (Figure 5b). A good overlap between the emission band of the donor (**D**) and the absorption band of the acceptor (**A**) and a higher extinction coefficient of the acceptor indicates a possible transfer of resonant excitation energy from the donor to the acceptor (Figure S8b in the Supporting Information).[22] When mixture **C** (1×10^{-5} M) was excited at $\lambda = 380$ nm, it showed a sharp decrease in the fluorescence emission at $\lambda = 457$ nm and an increase in intensity at $\lambda = 512$ nm. This indicates an energy transfer from **D** to **A** rather than direct excitation of the acceptor. Evidence of energy transfer was also obtained by comparing the emission of **A** excited directly at $\lambda = 420$ nm and the emission of **C** excited at $\lambda = 380$ nm (Figure 5c). The intensity of **C** excited at $\lambda = 380$ nm was greater than that of directly excited **A**, which indicates that the excitation energy is transferred from **D** to **A**. In toluene, **D** (1×10^{-5} M) showed emission maxima at $\lambda = 463$ and 489 nm, **A** (1×10^{-5} M) showed peaks at $\lambda = 526$ and 564 nm, and **C** (1×10^{-5} M) showed peaks at $\lambda = 465$ and 497 nm and a broad hump at $\lambda = 524$ nm (Figure S8c in the Supporting Information).

The extent of energy transfer was more pronounced in *n*-heptane than in toluene, as observed from the ratio of emission intensity at $\lambda = 457$ and 512 nm (Figure 5d). Because **C** forms a gel in *n*-heptane and not in toluene, the proximity between **D** and **A** should be greater in *n*-heptane due to hydrogen-bonding, π-stacking, and van der Waals interactions, and this should thus allow improved energy transfer. The solution of **D** in *n*-heptane was a light yellowish-green color, but **C** adopted the yellow color of **A** under normal daylight (Figure S8d in the Supporting Information). Also, under $\lambda = 365$ nm UV light, **D** showed sky-blue emission and **A** showed green emission. Mixture **C** exhibited green emission, which again indicates an energy transfer from **D** to **A**. On titration of **D** (1×10^{-5} M) with **A** in *n*-heptane, a progressive disappearance of the $\lambda = 457$ nm band was observed, which indicates greater extent of energy transfer (Figure 6a). Concentration-dependent emission spectra showed an optimum concentration of 5×10^{-5} M of **C** required for maximum energy transfer in n-heptane, at which the $\lambda = 457$ nm peak disappeared completely (Figure 6b).

The effect of temperature was also reflected in the aggregation patterns of **D** and **A** in *n*-heptane. When a solution of either **D** or **A** (2×10^{-5} M) was cooled from 65 to 10 °C,

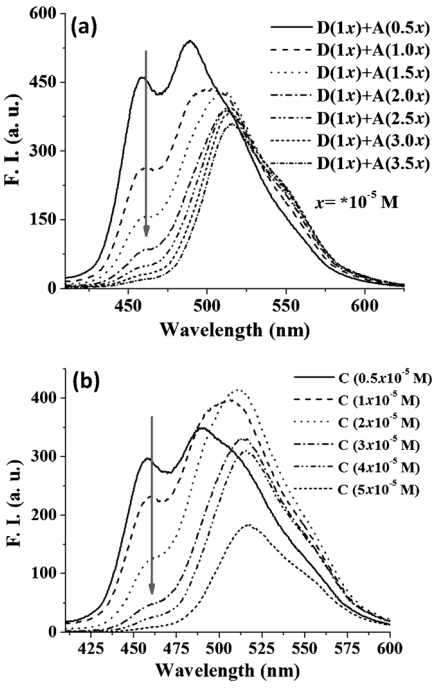

Figure 6. a) Titration of **D** with increasing quantities of **A** and b) emission spectra of incremental concentrations of **C** in *n*-heptane. $\lambda_{ex} = 380$ nm for both graphs.

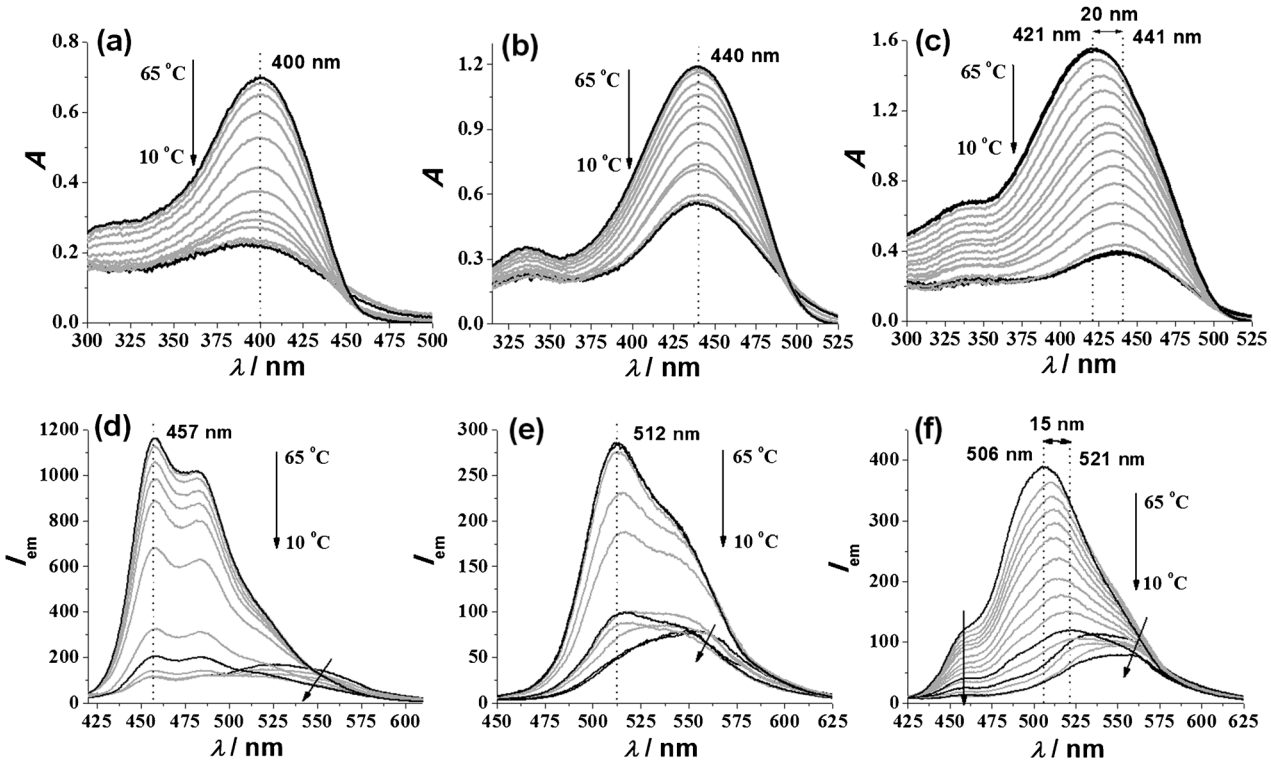

Figure 7. Absorption and emission spectra showing temperature-dependent aggregation of a,d) **D** (20 μM); b,e) **A** (20 μM); and c,f) **C** (20 μM of **D** + 20 μM of **A**) in *n*-heptane.

the intensity of the absorption maxima decreased, which indicates the appearance of an aggregated state (Figure 7).[17b] Interestingly, when **C** (2×10^{-5} M) was subjected to temperature variation, the intensity decreased, with a redshift of about 20 nm of the band that indicated a *J*-type aggregation[23] between **D** and **A**. This was also observed in the emission spectra under variable temperature conditions. A monomeric emission was observed at higher temperatures for **D** and **A** in *n*-heptane. The emission maximum showed an intensity loss upon a decrease in temperature and finally this reached an aggregated state showing emission at higher wavelengths ($\lambda\approx550$ nm). At higher temperatures, **C** showed an emission maximum at $\lambda=506$ nm with a small hump at $\lambda=457$ nm. Upon cooling, there was an intensity loss in the spectrum with a concomitant redshift (≈15 nm) of the emission band; this finally reached an aggregated state. This suggests that, upon cooling, the mixture first formed a primary *J*-type self-assembly followed by a secondary self-aggregation. It may be noted that the $\lambda=457$ nm band disappeared at lower temperatures, which indicates an increase in the energy transfer efficiency due to the association of **D** to **A** in close proximity.

Solvatochromism was observed for both **D** and **A** depending on the polarity of the organic solvents. The absorption maximum showed a redshift of about 8 nm for **D** and about 10 nm for **A** upon changing the solvent from *n*-heptane to chloroform (Figure S10 in the Supporting Information). The effect of solvent-induced shifts was more pronounced in the emission maxima than in the absorption maxima. This indicates that the effect of the solvent polarity was more pronounced in the excited state than in the ground state. Monotonous redshifts of the emission maxima of about 10 nm for **D** and about 35 nm for **A** were observed upon changing the solvent from *n*-heptane to chloroform (Figure 8). However, an abrupt change in the emission spectra, with a concomitant redshift and intensity loss, was observed in ethanol and acetonitrile for both **D** and **A**, most likely due to the self-aggregation process. Also, the redshift in the emission maxima was greater in **A** than in **D**, which suggests that the excited state of **A** is more sensitive to the solvent polarity than that of **D**. This could be explained from the calculated frontier molecular orbitals of the energy-minimized structures, which show that the lowest unoccupied molecular orbitals (LUMOs) are more polar than the corresponding highest occupied molecular orbitals (HOMOs). It is clear from the molecular structure of the gelators that through conjugation with the end functional group (ester) is possible only for **A** due to the presence of sp^2 carbons as linkers, and this is not possible for **D** (sp^3-hybridized linkers). Therefore, electron delocalization is restricted in the central TPV core in **D**. Thus, the calculated LUMO showed insignificant delocalized orbital contribution in the sp^3 centers in **D** but a significant delocalized orbital contribution in the sp^2 centers of **A**. This indicates that the LUMO of **A** is more polar than the LUMO of **D**. Thus, in a polar solvent, the LUMO of **A** should be more stabilized and this leads to a decrease in the HOMO–LUMO gap, which should result in an increase in the wavelength of the emission maximum (the redshifts).

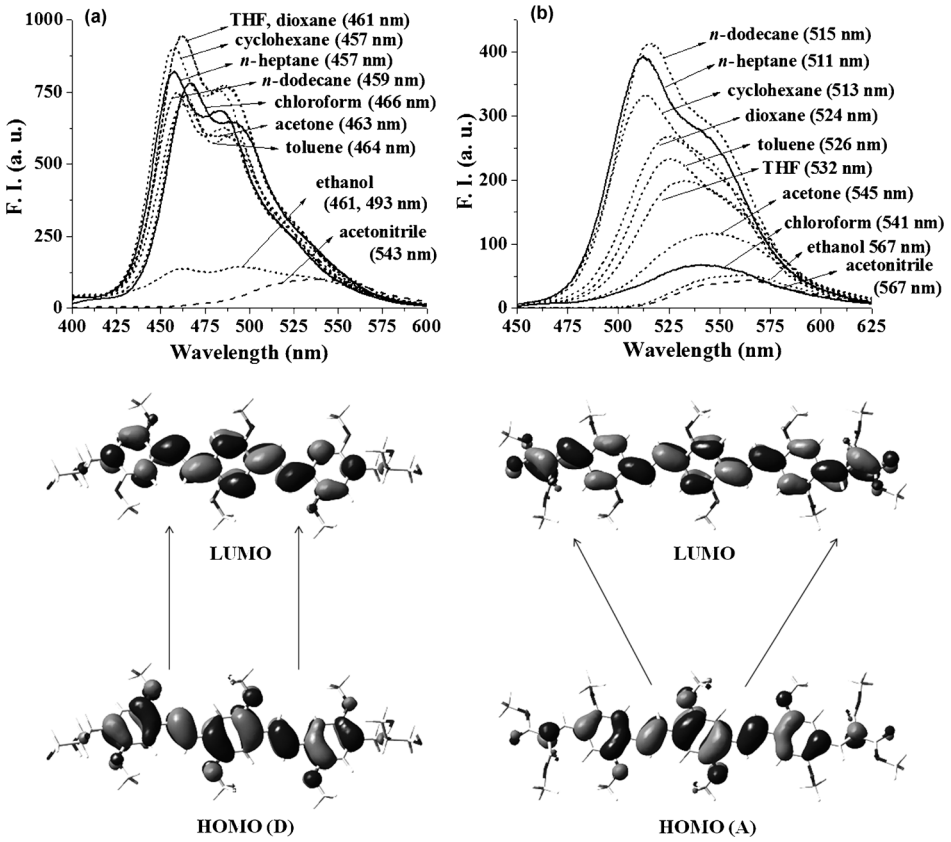

Figure 8. Solvatochromic effect of a) **D** and b) **A** under fluorescence spectroscopy. $[\mathbf{D}]=[\mathbf{A}]=1\times10^{-5}$ M in each case, $\lambda_{ex}=380$ nm for **D** and 420 nm for **A**. DFT B3YLP/6-31G* level single point energy calculations of **D** and **A** in *n*-heptane using PCM solvent model. For simplicity in computation, the *n*-hexadecyloxy side-chains were replaced with methoxy groups. Arrows indicate the charge delocalization.

However, this effect would be less pronounced in **D**, which clearly matches with the experimental observations.

To establish a light-harvesting array, we chose two known dyes, that is, anthracene (**N**) and rhodamine 6G (**R**; Scheme 1), because their emission and absorption spectra provide a significant overlap along a particular order of the probes and the two complementary gelators, **N**-**D**-**A**-**R** (Figure S11a in the Supporting Information). We have already shown that due to the presence of ground-state interaction between **D** and **A**, the individual absorption maximum merged into a single absorption maximum. However, this kind of ground-state interaction was not observed in any combination of the four chromophores except **D** and **A** only (Figure S11b in the Supporting Information).

Figure 9a showed a stepwise addition of all the four chromophores together to achieve a stepwise energy transfer in the assembly. When **N** (5×10^{-4} M) was excited at $\lambda=356$ nm, it showed an emission maximum at $\lambda=400$ nm. Addition of **D** (5×10^{-5} M) showed effective quenching of the emission at $\lambda=400$ nm and resulted in new emission maxima at $\lambda=461$ and 486 nm. Due to the weak emissive property of **N**, a ten-fold excess was used relative to **D**. This indicated transfer of the excitation energy from **N** to **D**. A ternary mixture of **N**+**D**+**A** (10:1:1) showed an emission maximum at $\lambda=518$ nm and the mixture of all four chromophores **N**+**D**+**A**+**R** (10:1:1:1 molar ratio) exhibited only one emission maximum at $\lambda=565$ nm when excited at $\lambda=356$ nm. Thus each new addition of an individual chromophore led to a quantitative energy transfer to the higher wavelength, which finally accumulated at that of **R**. The corresponding excitation spectra at the respective emission maxima is shown in Figure S12 (see the Supporting Information). Interestingly, in this light-harvesting assembly that contains **N-D-A-R**, excitation at any point in the whole spectral region showed a single emission at **R** (Figure 9b). A remarkable shift in λ_{max} ($\lambda\approx210$ nm) was obtained when the assembly was excited at $\lambda=356$ nm. This resulted in the emission at **R** ($\lambda=566$ nm), which indicates efficient light harvesting. However, the emission intensity could be tuned depending on a multitude of factors, including the excitation wavelength of the donor, the distance from the donor to the final acceptor (**R**) in the sequence, the overlap integral, the quantum efficiency of the donor, the extinction coefficient of the acceptor, and the interaction between the donors and **R**.[22] Thus, the emission intensity of **R** increased on approaching the excitation wavelength from **N** to **R**. Interestingly, the color of the solution shifted accordingly on successive addition of different chromophores in that particular order. Visual examination showed the solution of **N** to be colorless, **N**+**D** to be greenish-yellow, **N**+**D**+**A** to be deep yellow, and **N**+**D**+**A**+**R** to be reddish-orange under normal daylight (Figure 9c). When the respective mixtures were observed under $\lambda=365$ nm UV light, they showed a blue emission for **N**, a sky-blue emission for **N**+**D**, a green emission for **N**+**D**+**A**, and a reddish-orange emission for **N**+**D**+**A**+**R**. Note that an almost quantitative efficiency in energy transfer was obtained in solution only at 5×10^{-5} M. This is due to the efficient π-stacking interactions between the molecules aided by van der Waals and hydrogen-bonding interactions between **D** and **A** in *n*-heptane. This can be anticipated from the observation that **R** alone precipitated readily from *n*-heptane within a few minutes, whereas it remained in solution along with the assembly for a number of days.

To establish the participation of each chromophore in the assembly as a stepping stone for energy transfer, we performed a number of control experiments. Concentrations of

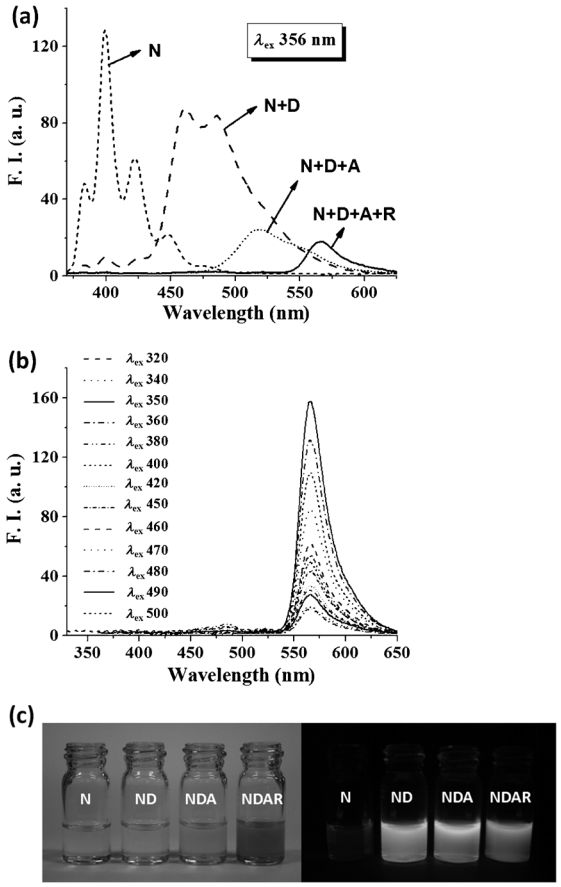

Figure 9. a) Stepwise energy transfer in the assembly of **N**-**D**-**A**-**R** excited at $\lambda = 356$ nm. b) Emission spectra of the **N**-**D**-**A**-**R** mixture at different wavelengths. c) The same solutions under normal daylight and $\lambda = 365$ nm UV light. $[\mathbf{N}] = 5\times10^{-4}$ M and $[\mathbf{D}] = [\mathbf{A}] = [\mathbf{R}] = 5\times10^{-5}$ M in *n*-heptane in each case. (A colored version of Figure 9c is available in the Supporting Information).

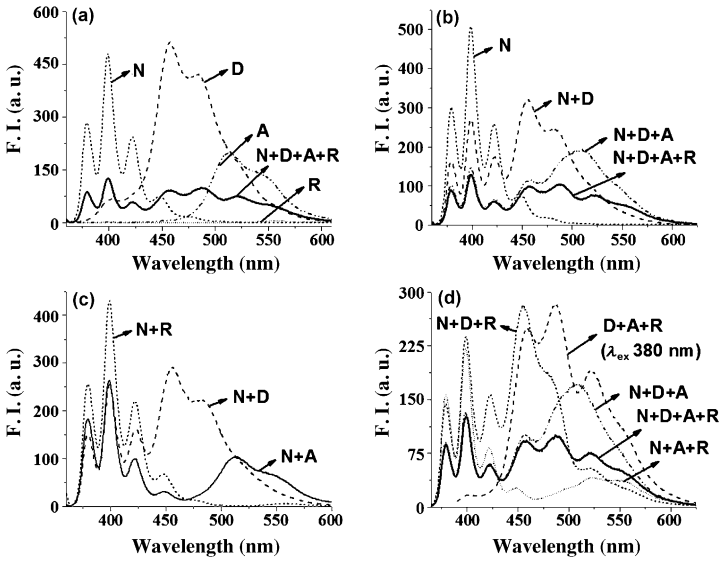

Figure 10. Emission spectra showing a) individual chromophores and the **N**+**D**+**A**+**R** mixture, b) the stepwise energy transfer, c) the energy transfer efficiency from **N** to **D**, **A**, and **R**, and d) termination of energy transfer with elimination of **D** or **A** from the assembly in *n*-heptane at $\lambda = 356$ nm excitation. $[\mathbf{N}] = 1\times10^{-4}$ M and $[\mathbf{D}] = [\mathbf{A}] = [\mathbf{R}] = 1\times10^{-5}$ M in each case.

5×10^{-4} M for **N** and 5×10^{-5} M for **D**, **A**, and **R** were chosen because the variable-concentration emission spectra of the mixtures of **N**+**D**, **D**+**A**, or **A**+**R** showed a complete energy transfer at these concentrations (Figure 6b and Figure S13 in the Supporting Information). Also, the variable-concentration emission spectra of the mixture of all four chromophores showed an efficient energy transfer at the above concentrations. The rate of energy transfer (k_{ET}; 3.6×10^{13} $M^{-1}S^{-1}$ for **N** to **D**, 1.7×10^{14} $M^{-1}S^{-1}$ for **D** to **A** and 4.7×10^{14} $M^{-1}S^{-1}$ for **A** to **R**) was calculated by using the Stern–Volmer constants (k_{SV}; 1.3×10^{5} M^{-1} for **N**+**D**, 2.5×10^{5} M^{-1} for **D**+**A**, 4.7×10^{5} M^{-1} for **A**+**R**) and the individual lifetimes (Figure S14 and Table S1 in the Supporting Information).[24]

For the control experiment, fivefold diluted solutions were used to gain a better understanding of the role of each chromophore. The individual emission band due to each of the four chromophores was clearly distinguishable in the assembly in these diluted solutions. When the individual chromophores were excited at $\lambda = 356$ nm they showed the respective emission spectra due to the residual absorbance at $\lambda = 356$ nm (Figure 10a). Chromophore **R** showed negligible emission when excited at $\lambda = 356$ nm. A mixture of all four chromophores showed loss in the emission intensity for **N**, **D**, and **A** and accumulated at **R**, which was more prominent at increased concentrations (Figure S13c in the Supporting Information). The stepwise energy transfer was also demonstrated at this lower concentration. Chromophore **N** alone (1×10^{-4} M) showed an emission maximum at $\lambda = 400$ nm when excited at $\lambda = 356$ nm in *n*-heptane (Figure 10b). Addition of **D** (1×10^{-5} M) to the solution of **N** resulted in a decrease in the intensity of **N** at $\lambda = 400$ nm and the emission intensity accumulated at $\lambda = 455$ nm. The ternary complex after addition of **A** (1×10^{-5} M) led to a further loss in fluorescence emission intensity at $\lambda = 400$ and also at 455 nm, and showed a maximum emission at $\lambda = 508$ nm due to **A**. Finally, addition of **R** (1×10^{-5} M) extracted the energy from the assembly, leading to an intensity loss of **A** at $\lambda = 508$ nm. However, due to the low emissive nature of **R** in *n*-heptane, the emission intensity was not so prominent at this concentration. Furthermore, it should be mentioned that a complete energy transfer from **N** to **D** did not lead to amplified emission because of the low emissive nature of **N**. Also, the ratio of **D**/**A** and **A**/**R** was 1:1 in both cases, which indicates that an excess of the acceptor is required for complete energy transfer.

Thus, a mixture of **N** and **D** shows an emission at **D** ($\lambda =$ 455 nm) upon excitation at $\lambda = 356$ nm (Figure 10c). A lesser extent of energy transfer was also observed from **N** to **A** due to the spectral overlap of the emission of **N** and absorption of **A**. However, a negligible energy transfer from **N** to **R** was observed due to the lack of spectral overlap. The efficiency of energy transfer should be reduced if one or two chromophores are removed from the **N**-**D**-**A**-**R** array. Thus,

elimination of **A** from the assembly showed discontinuation of the energy transfer to **R** and the emission accumulated at $\lambda = 455$ nm (Figure 10d). A mixture of **N**+**D**+**A** showed emission at **A** ($\lambda = 508$ nm). However, elimination of **D** revealed a lesser extent of energy transfer from **N** to **R** due to the spectral overlap between **N** and **A**, as mentioned earlier. The emission intensity of the mixture of **N**, **D**, and **A** appeared at $\lambda = 508$ nm due to the continuation of the array. Also, the mixture of **D**, **A**, and **R** showed greater emission intensity when excited at $\lambda = 380$ nm due to the high emissive nature of **D**.

Energy transfer was also observed in the solid state, in a thin film prepared on a quartz plate using a front-face geometry.[24c] When excited at $\lambda = 356$ nm, **N** exhibited an emission maximum at $\lambda = 420$ nm (Figure 11a). The mixture

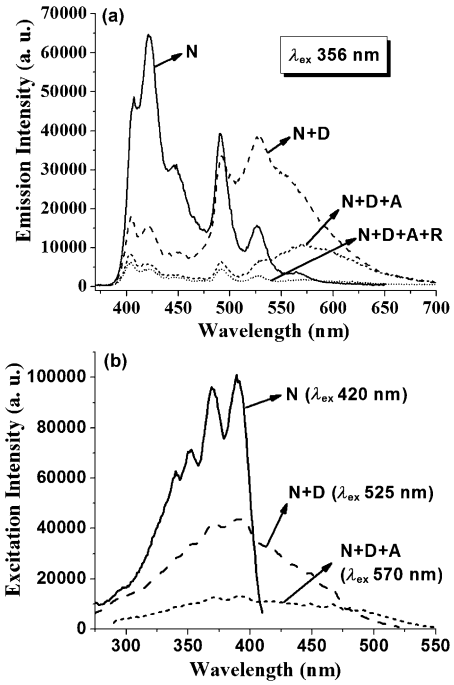

Figure 11. a) Emission and b) excitation spectra of the assembly of **N**, **D**, **A**, and **R** in the solid state.

of **N** and **D** (10:1 molar ratio) showed an emission maximum at $\lambda = 528$ nm. The ternary complex of **N**, **D**, and **A** (10:1:1) showed an emission at $\lambda = 568$ nm. However, a mixture of all the four chromophores (10:1:1:1) quenched the emission due to the non-emissive nature of **R** in the solid state. Thus **R** acted as an energy sink in the solid state. The corresponding excitation spectra at their respective emission maxima showed that the excitation maximum was located near
$\lambda = 380$ nm (Figure 11b). However, the excitation spectra gradually became broader on progressive doping of **D** and **A** with **N**.

To probe the cascade energy transfer, lifetime measurements were performed in *n*-heptane by using 5×10^{-4} M **N** and 5×10^{-5} M **D**, **A**, and **R** (Figure S15 in the Supporting Information). Lifetimes of the individual compounds are listed in the Table S2 (see the Supporting Information). Lifetimes of the assembly of **N**, **D**, **A**, and **R** were also recorded in solution and as a thin film, and the efficiency for the cascade energy transfer was estimated. In solution, **N** showed a monoexponential decay with a time constant of 3.6 ns when the emission was recorded at $\lambda = 400$ nm. Addition of **D** to the solution of **N** induced a decrease in the lifetime of **N** with the average lifetime (τ_{av}) of 3.3 ns, which indicated an energy transfer efficiency of only 8% (Table S3 in the Supporting Information). However, at this concentration the energy transfer reached its optimum and, therefore, addition of **A** into this mixture (**N**+**D**) did not result in any further decrease in the lifetime of **N**. However, in a thin film, the assembly showed a progressive decrease in the lifetime of **N** (emission recorded at $\lambda = 420$ nm), which indicated a continuous unidirectional energy transfer from **N** to **R**. In the thin film, **N** alone showed a bi-exponential decay with the average lifetime of 2.3 ns, which showed an energy transfer of 9% upon addition of **D** (**N**+**D**), 13% upon addition of **A** (**N**+**D**+**A**), and up to 43% upon addition of **R** (**N**+**D**+**A**+**R**; Table S4 in the Supporting Information). This indicates that the process of energy transfer occurs through the Förster pathway, in which the excitation energy of **N** migrates to **R** through **D** and **A**. Although evidence of energy transfer was observed in both solution and a thin film, the efficiency of the energy transfer is greater in the thin film.[15,24c]

Therefore, all the results obtained herein supported the construction of an effective energy transfer assembly. The energy transfer occurs from **N** to **R** via **D** and **A** when the first donor (**N**) in the assembly is excited. Figure 12 shows a

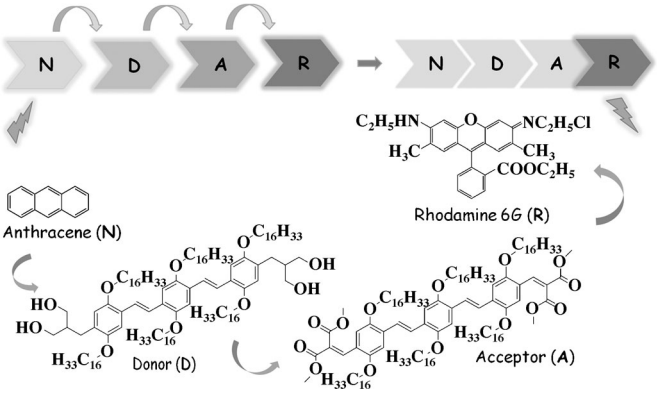

Figure 12. Proposed model depicting the phenomenon of energy transfer through donor–acceptor interactions between the chromophores.

model that depicts the process of energy transfer through the association of four chromophores. The individual chromophores are luminescent in nature. When they are brought together, they show energy transfer in a particular order depending on their spectral overlap. Also, elimination of any chromophore from the assembly leads to the disruption of the cascade energy transfer.

Conclusion

In summary, two new low-molecular-mass organogelators based on the tri-*p*-phenylene vinylene skeleton have been developed. The intergelator interactions manifest a donor–acceptor molecular assembly, which in turn controls their macroscopic properties. Intermolecular hydrogen-bonding, π-stacking, and van der Waals interactions operate in the donor and acceptor mixture, which leads them to form a gel. The photochromic nature of this class of molecules showed evidence of ground-state interactions between the donor and the acceptor. Efficient energy transfer was observed in the donor–acceptor assembly in solution. In conjunction with two more chromophores, that is, anthracene and rhodamine 6G, cascade energy transfer was observed in the assembly. This allowed the construction of a wide-range light-harvesting assembly, which on excitation at one end produced emission at the other end of the series. Dealing with these factors is a route to build up highly efficient light-harvesting assemblies that can be applied in photonic devices and solar cells.

Acknowledgements

We thank the Department of Science and Technology (J.C. Bose fellowship to S.B.) for financial support, the Institute Nanoscience Initiative at IISc and the Raman Research Institute for various instrumental facilities, and Dr. Subi J. George for helpful discussions. S.K.S. is grateful to the CSIR for a senior research fellowship and IISc for a postdoctoral research associateship. We thank Prof. S. Vasudevan of the Department of Inorganic and Physical Chemistry, IISc, for help with the lifetime measurements.

[1] a) W. Kühlbrandt, D. N. Wang, Y. Fujiyoshi, *Nature* **1994**, *367*, 614–621; b) G. McDermott, S. M. Prince, A. A. Freer, A. M. Hawthornthwaite-Lawless, M. Z. Papiz, R. J. Cogdell, N. W. Isaacs, *Nature* **1995**, *374*, 517–521; c) X. Hu, A. Damjanovic, T. Ritz, K. Schulten, *Proc. Natl. Acad. Sci. USA* **1998**, *95*, 5935–5941.

[2] a) *Energy Harvesting Materials* (Ed.: D. L. Andrews), World Scientific, Singapore, **2005**; b) J. L. Sessler, B. Wang, A. Harriman, *J. Am. Chem. Soc.* **1995**, *117*, 704–714; c) R. Ziessel, A. Harriman, *Chem. Commun.* **2011**, *47*, 611–631; d) N. H. Damrauer, J. M. Hodgkiss, J. Rosenthal, D. G. Nocera, *J. Phys. Chem. B* **2004**, *108*, 6315–6321; e) J. M. Hodgkiss, N. H. Damrauer, S. Presse, J. Rosenthal, D. G. Nocera, *J. Phys. Chem. B* **2006**, *110*, 18853–18858.

[3] a) M.-S. Choi, T. Yamazaki, I. Yamazaki, T. Aida, *Angew. Chem.* **2004**, *116*, 152–160; *Angew. Chem. Int. Ed.* **2004**, *43*, 150–158; b) V. Balzani, P. Ceroni, M. Maestri, V. Vicinelli, *Curr. Opin. Chem. Biol.* **2003**, *7*, 657–665; c) D. Liu, S. de Feyter, M. Cotlet, A. Stefan, U.-M. Wiesler, A. Herrmann, D. Grebel-Koehler, J. Qu, K. Mullen, F. C. De Schryver, *Macromolecules* **2003**, *36*, 5918–5925; d) S. Hecht, J. M. J. Frechet, *Angew. Chem.* **2001**, *113*, 76–94; *Angew. Chem. Int. Ed.* **2001**, *40*, 74–91; e) C. Röger, M. G. Muller, M. Lysetska, Y. Miloslavina, A. R. Holzwarth, F. Wurthner, *J. Am. Chem. Soc.* **2006**, *128*, 6542–6543; f) T. S. Balaban, *Acc. Chem. Res.* **2005**, *38*, 612; g) K. Becker, J. M. Lupton, J. Feldmann, S. Setayesh, A. C. Grimsdale, K. Mullen, *J. Am. Chem. Soc.* **2006**, *128*, 680–681; h) Y.-J. Cheng, T.-Y. Luh, *Chem. Eur. J.* **2004**, *10*, 5361–5368; i) G. Calzaferri, S. Huber, H. Maas, C. Minkowski, *Angew. Chem.* **2003**, *115*, 3860–3888; *Angew. Chem. Int. Ed.* **2003**, *42*, 3732–3758; j) T.-Q. Nguyen, J. Wu, V. Doan, B. J. Schwartz, S. H. Tolbert, *Science* **2000**, *288*, 652–656; k) R. D. Fossum, M. A. Fox, A. M. Gelormini, A. J. Pearson, *J. Phys. Chem. B* **1997**, *101*, 2526–2532.

[4] a) S. Prathapan, T. N. Johnson, J. S. Lindsey, *J. Am. Chem. Soc.* **1993**, *115*, 7519–7520; b) K.-Y. Tomizaki, R. S. Loewe, C. Kirmaier, J. K. Schwartz, J. L. Retsek, D. F. Bocian, D. Holten, J. S. Lindsey, *J. Org. Chem.* **2002**, *67*, 6519–6534; c) A. Nakano, A. Osuka, I. Yamazaki, T. Yamazaki, Y. Nishimura, *Angew. Chem.* **1998**, *110*, 3172–3176; *Angew. Chem. Int. Ed.* **1998**, *37*, 3023–3027; d) H. S. Cho, H. Rhee, J. K. Song, C. K. Min, M. Takase, N. Aratani, S. Cho, A. Osuka, T. Joo, D. Kim, *J. Am. Chem. Soc.* **2003**, *125*, 5849–5860; e) C. V. K. Sharma, G. A. Broker, J. G. Huddleston, J. W. Baldwin, R. M. Metzger, R. D. Rogers, *J. Am. Chem. Soc.* **1999**, *121*, 1137–1144; f) N. Sakai, R. S. K. Kishore, S. Matile, *Org. Biomol. Chem.* **2008**, *6*, 3970–3976; g) X. Yang, R. Lu, P. Xue, B. Li, D. Xu, T. Xu, Y. Zhao, *Langmuir* **2008**, *24*, 13730–13735.

[5] a) C. A. Hunter, R. K. Hyde, *Angew. Chem.* **1996**, *108*, 2064–2067; *Angew. Chem. Int. Ed. Engl.* **1996**, *35*, 1936–1939; b) R. Takahashi, Y. Kobuke, *J. Am. Chem. Soc.* **2003**, *125*, 2372–2373; c) T. S. Balaban, R. Goddard, M. Linke-Schaetzel, J.-M. Lehn, *J. Am. Chem. Soc.* **2003**, *125*, 4233–4239; d) M. D. Ward, *Chem. Soc. Rev.* **1997**, *26*, 365–375; e) T. Pons, I. L. Medintz, X. Wang, D. S. English, H. Mattoussi, *J. Am. Chem. Soc.* **2006**, *128*, 15324–15331; f) E. S. Barrett, T. J. Dale, J. Rebek, *J. Am. Chem. Soc.* **2007**, *129*, 8818–8824; g) C. V. Kumar, M. R. Duff, *Photochem. Photobiol. Sci.* **2008**, *7*, 1522–1530; h) M. Takahashi, N. Nishizawa, S. Ohno, M. Kakita, N. Fujita, M. Yamashita, T. Sengoku, H. Yoda, *Tetrahedron* **2009**, *65*, 2669–2677; i) I. Place, T. L. Penner, D. W. McBranch, D. G. Whitten, *J. Phys. Chem. A* **2003**, *107*, 3169–3177.

[6] a) C. Devadoss, P. Bharathi, J. S. Moore, *J. Am. Chem. Soc.* **1996**, *118*, 9635–9644; b) D.-L. Jiang, T. Aida, *Nature* **1997**, *388*, 454–456; c) M.-S. Choi, T. Aida, T. Yamazaki, I. Yamazaki, *Angew. Chem.* **2001**, *113*, 3294–3298; *Angew. Chem. Int. Ed.* **2001**, *40*, 3194–3198; d) A. Adronov, J. M. Frechet, *Chem. Commun.* **2000**, 1701–1710; e) J. M. Serin, D. W. Brousmiche, J. M. Frechet, *J. Am. Chem. Soc.* **2002**, *124*, 11848–11849; f) V. Vicinelli, P. Ceroni, M. Maestri, V. Balzani, M. Gorka, F. Vogtle, *J. Am. Chem. Soc.* **2002**, *124*, 6461–6468; g) Y. Zeng, Y. Li, M. Li, G. Yang, Y. Li, *J. Am. Chem. Soc.* **2009**, *131*, 9100–9106.

[7] a) N. Kimizuka, T. Kunitake, *J. Am. Chem. Soc.* **1989**, *111*, 3758–3759; b) L. A. J. Chrisstoffels, A. Adronov, J. M. Frechet, *Angew. Chem.* **2000**, *112*, 2247–2251; *Angew. Chem. Int. Ed.* **2000**, *39*, 2163–2167; c) C. Röger, Y. Miloslavina, D. Brunner, A. R. Holzwarth, F. Wurthner, *J. Am. Chem. Soc.* **2008**, *130*, 5929–5939; d) T. Ishi-i, K.-i. Murakami, Y. Imai, S. Mataka, *J. Org. Chem.* **2006**, *71*, 5752–5760.

[8] a) A. Kraft, A. C. Grimsdale, A. B. Holmes, *Angew. Chem.* **1998**, *110*, 416–443; *Angew. Chem. Int. Ed.* **1998**, *37*, 402–428; b) U. Mitschke, P. Bauerle, *J. Mater. Chem.* **2000**, *10*, 1471–1507; c) G. Yu, J. Gao, J. C. Hummelen, F. Wudl, A. J. Heeger, *Science* **1995**, *270*, 1789–1791; d) J. J. M. Halls, C. A. Walsh, N. C. Greenham, E. A. Marseglia, R. H. Friend, *Nature* **1995**, *376*, 498–500; e) T.-C. Liang, I.-H. Chiang, P.-J. Yang, D. Kekuda, C.-W. Chu, H.-C. Lin, *J. Polym. Sci. Part A J. Pol. Sci.: Part A: Pol. Chem.* **2009**, *47*, 5998–6013; f) B. Zhang, X. Chen, J. Yang, D. Yu, Y. Chen, D. Wu, R. Fu, M. Zhang, *Nanotechnology* **2010**, *21*, 045601 (7pp); g) Y. Ooyama, A. Ishii, Y. Kagawa, I. Imae, Y. Harima, *New J. Chem.* **2007**, *31*, 2076–2082.

[9] a) P. Terech, R. G. Weiss, *Chem. Rev.* **1997**, *97*, 3133–3159; b) T. Ishi-I, S. Shinkai, *Top. Curr. Chem.* **2005**, *258*, 119–160; c) A. Ajayaghosh, V. K. Praveen, *Acc. Chem. Res.* **2007**, *40*, 644–656; d) A. Pal, H. Basit, S. Sen, V. K. Aswal, S. Bhattacharya, *J. Mater. Chem.* **2009**, *19*, 4325–4334.

[10] a) M. Montalti, L. S. Dolci, L. Prodi, N. Zaccheroni, M. C. A. Stuart, K. J. C. van Bommel, A. Friggeri, *Langmuir* **2006**, *22*, 2299–2303; b) A. D. Del Guerzo, A. G. L. Olive, J. Reichwagen, H. Hopf, J.-P. Desvergne, *J. Am. Chem. Soc.* **2005**, *127*, 17984–17985; c) J.-H. Ryu, M. Lee, *J. Am. Chem. Soc.* **2005**, *127*, 14170–14171; d) S. Yamaguchi, I. Yoshimura, T. Kohira, S.-i. Tamaru, I. Hamachi, *J. Am. Chem. Soc.* **2005**, *127*, 11835–11841; e) J. B. Beck, S. J. Rowan, *J. Am. Chem. Soc.* **2003**, *125*, 13922–13923; f) T. Nakashima, N. Kimizuka, *Adv. Mater.* **2002**, *14*, 1113–1116; g) T. Sagawa, S. Fukugawa, T.

Yamada, H. Ihara, *Langmuir* **2002**, *18*, 7223–7228; h) K. V. Rao, K. K. R. Datta, M. Eswaramoorthy, S. J. George, *Angew. Chem.* **2011**, *123*, 1211–1216; *Angew. Chem. Int. Ed.* **2011**, *50*, 1179–1184.

[11] a) M. Ikeda, M. Takeuchi, S. Shinkai, *Chem. Commun.* **2003**, 1354–1355; b) L. A. Estroff, A. D. Hamilton, *Chem. Rev.* **2004**, *104*, 1201–1217; c) J. F. Hulvat, M. Sofos, K. Tajima, S. I. Stupp, *J. Am. Chem. Soc.* **2005**, *127*, 366–372; d) E. Lee, J.-K. Kim, M. Lee, *Angew. Chem.* **2008**, *120*, 6475–6478; *Angew. Chem. Int. Ed.* **2008**, *47*, 6375–6378; e) K. V. Rao, K. Jayaramulu, T. K. Maji, S. J. George, *Angew. Chem.* **2010**, *122*, 4314–4318; *Angew. Chem. Int. Ed.* **2010**, *49*, 4218–4222.

[12] a) F. J. M. Hoeben, I. O. Shklyarevskiy, M. J. Pouderoijen, H. Engelkamp, A. P. H. J. Schenning, P. C. M. Christianen, J. C. Maan, E. W. Meijer, *Angew. Chem.* **2006**, *118*, 1254–1258; *Angew. Chem. Int. Ed.* **2006**, *45*, 1232–1236; b) J. Zhang, F. J. M. Hoeben, M. J. Pouderoijen, A. P. H. J. Schenning, E. W. Meijer, F. C. De Schryver, S. de Feyter, *Chem. Eur. J.* **2006**, *12*, 9046–9055; c) F. J. M. Hoeben, M. Wolffs, J. Zhang, S. D. Feyter, P. Leclere, A. P. H. J. Schenning, E. W. Meijer, *Angew. Chem.* **2004**, *116*, 2010–2013; *Angew. Chem. Int. Ed.* **2004**, *43*, 1976–1979; d) A. P. H. J. Schenning, E. Peeters, E. W. Meijer, *J. Am. Chem. Soc.* **2000**, *122*, 4489–4495.

[13] a) A. Ajayaghosh, S. J. George, *J. Am. Chem. Soc.* **2001**, *123*, 5148–5149; b) V. K. Praveen, S. J. George, R. Varghese, C. Vijayakumar, A. Ajayaghosh, *J. Am. Chem. Soc.* **2006**, *128*, 7542–7550; c) C. Vijayakumar, V. K. Praveen, K. K. Kartha, A. Ajayaghosh, *Phys. Chem. Chem. Phys.* **2011**, *13*, 4942–4949; d) A. Ajayaghosh, V. K. Praveen, S. Srinivasan, R. Varghese, *Adv. Mater.* **2007**, *19*, 411–415; e) A. Ajayaghosh, V. K. Praveen, C. Vijayakumar, *Chem. Soc. Rev.* **2008**, *37*, 109–122.

[14] a) A. Ajayaghosh, V. K. Praveen, C. Vijayakumar, S. J. George, *Angew. Chem.* **2007**, *119*, 6376–6381; *Angew. Chem. Int. Ed.* **2007**, *46*, 6260–6265; b) X. Zhang, Z.-K. Chen, K. P. Loh, *J. Am. Chem. Soc.* **2009**, *131*, 7210–7211; c) L. Chen, S. Revel, K. Morris, D. J. Adams, *Chem. Commun.* **2010**, *46*, 4267–4269.

[15] a) K. Sugiyasu, N. Fujita, S. Shinkai, *Angew. Chem.* **2004**, *116*, 1249–1253; *Angew. Chem. Int. Ed.* **2004**, *43*, 1229–1233; b) T. Shu, J. Wu, M. Lu, L. Chen, T. Yi, F. Li, C. Huanga, *J. Mater. Chem.* **2008**, *18*, 886–893; c) C.-H. Chen, K.-Y. Liu, S. Sudhakar, T.-S. Lim, W. Fann, C.-P. Hsu, T.-Y. Luh, *J. Phys. Chem. B* **2005**, *109*, 17887–17891; d) R. Abbel, R. van der Weegen, W. Pisula, M. Surin, P. Leclere, R. Lazzaroni, E. W. Meijer, A. P. H. J. Schenning, *Chem. Eur. J.* **2009**, *15*, 9737–9746; e) R. Abbel, R. van der Weegen, E. W. Meijer, A. P. H. J. Schenning, *Chem. Commun.* **2009**, 1697–1699; f) M. Wolffs, F. J. M. Hoeben, E. H. A. Beckers, A. P. H. J. Schenning, E. W. Meijer, *J. Am. Chem. Soc.* **2005**, *127*, 13484–13485; g) F. J. M. Hoeben, M. Wolffs, J. Zhang, S. D. Feyter, P. Leclere, A. P. H. J. Schenning, E. W. Meijer, *J. Am. Chem. Soc.* **2007**, *129*, 9819–9828; h) A. Sautter, B. K. Kaletas, D. G. Schmid, R. Dobrawa, M. Zimine, G. Jung, I. H. M. van Stokkum, L. D. Cola, R. M. Williams, F. Wurthner, *J. Am. Chem. Soc.* **2005**, *127*, 6719–6729; i) J. M. Serin, D. W. Brousmiche, J. M. J. Frechet, *Chem. Commun.* **2002**, 2605–2607; j) K. Tsubaki, K. Takaishi, D. Sue, K. Matsuda, Y. Kanemitsu, T. Kawabata, *J. Org. Chem.* **2008**, *73*, 4279–4282; k) T.-W. Lee, O. O. Park, H. N. Cho, J.-M. Hong, C. Y. Kim, Y. C. Kim, *Synth. Met.* **2001**, *122*, 437–441; l) T.-W. Lee, O. O. Park, H. N. Cho, Y. C. Kim, *Synth. Met.* **2002**, *131*, 129–133.

[16] S. Bhattacharya, S. K. Samanta, *Langmuir* **2009**, *25*, 8378–8381.

[17] a) B. Wang, M. R. Wasielewski, *J. Am. Chem. Soc.* **1997**, *119*, 12–21; b) S. K. Samanta, A. Pal, S. Bhattacharya, *Langmuir* **2009**, *25*, 8567–8578.

[18] a) A. Pal, Y. K. Ghosh, S. Bhattacharya, *Tetrahedron* **2007**, *63*, 7334–7348; b) S. Bhattacharya, S. N. G. Acharya, A. R. Raju, *Chem. Commun.* **1996**, 2101–2102; c) S. Bhattacharya, S. N. G. Acharya, *Chem. Mater.* **1999**, *11*, 3121–3132.

[19] a) H. A. Barnes in *A Handbook of Elementary Rheology*, University of Wales, Institute of Non-Newtonian Fluid Mechanics, Aberystwyth, **2000**, pp. 55–61; b) F. M. Menger, K. L. Caran, *J. Am. Chem. Soc.* **2000**, *122*, 11679–11691; c) P. Terech, D. Pasquier, V. Bordas, C. Rossat, *Langmuir* **2000**, *16*, 4485–4494.

[20] a) S. K. Samanta, A. Pal, S. Bhattacharya, C. N. R. Rao, *J. Mater. Chem.* **2010**, *20*, 6881–6890; b) S. K. Samanta, A. Gomathi, S. Bhattacharya, C. N. R. Rao, *Langmuir* **2010**, *26*, 12230–12236; c) S. K. Samanta, K. S. Subrahmanyam, S. Bhattacharya, C. N. R. Rao, *Chem. Eur. J.* **2012**, *18*, 2890–2901.

[21] a) Y. Tang, E. H. Hill, Z. Zhou, D. G. Evans, K. S. Schanze, D. G. Whitten, *Langmuir* **2011**, *27*, 4945–4955; b) M. Mba, A. Moretto, L. Armelao, M. Crisma, C. Toniolo, M. Maggini, *Chem. Eur. J.* **2011**, *17*, 2044–2047; c) E. H. A. Beckers, P. Jonkheijm, A. P. H. J. Schenning, S. C. J. Meskers, R. A. J. Janssen, *ChemPhysChem* **2005**, *6*, 2029–2031; d) C. A. Sierra, P. M. Lahti, *J. Phys. Chem. A* **2006**, *110*, 12081–12088; e) E. H. A. Beckers, S. C. J. Meskers, A. P. H. J. Schenning, Z. Chen, F. Wurthner, P. Marsal, D. Beljonne, J. Cornil, R. A. J. Janssen, *J. Am. Chem. Soc.* **2006**, *128*, 649–657.

[22] J. R. Lakowicz, *Principles of Fluorescence Spectroscopy*, 2nd ed., Kluwer Academic/Plenum, New York, **1999**.

[23] a) S. Ghosh, X.-Q. Li, V. Stepanenko, F. Wurthner, *Chem. Eur. J.* **2008**, *14*, 11343–11357; b) F. Würthner, T. E. Kaiser, C. R. Saha-Moller, *Angew. Chem.* **2011**, *123*, 3436–3473; *Angew. Chem. Int. Ed.* **2011**, *50*, 3376–3410; c) M. Shirakawa, S.-i. Kawano, N. Fujita, K. Sada, S. Shinkai, *J. Org. Chem.* **2003**, *68*, 5037–5044; d) H. Wu, L. Xue, Y. Shi, Y. Chen, X. Li, *Langmuir* **2011**, *27*, 3074–3082; e) X.-Q. Li, X. Zhang, S. Ghosh, F. Wurthner, *Chem. Eur. J.* **2008**, *14*, 8074–8078.

[24] a) A. P. H. J. Schenning, J. v. Herrikhuyzen, P. Jonkheijm, Z. Chen, F. Wurthner, E. W. Meijer, *J. Am. Chem. Soc.* **2002**, *124*, 10252–10253; b) R. Abbel, C. Grenier, M. J. Pouderoijen, J. W. Stouwdam, P. E. L. G. Leclere, R. P. Sijbesma, E. W. Meijer, A. P. H. J. Schenning, *J. Am. Chem. Soc.* **2009**, *131*, 833–843; c) A. Ajayaghosh, S. J. George, V. K. Praveen, *Angew. Chem.* **2003**, *115*, 346–349; *Angew. Chem. Int. Ed.* **2003**, *42*, 332–335.

Received: December 12, 2011
Revised: July 13, 2012
Published online: October 16, 2012

